MIT Open Access Articles

Vascular Regeneration by Local Growth Factor Release Is Self-Limited by Microvascular Clearance

Massachusetts Institute of Technology

Vascular Regeneration by Local Growth Factor Release Is Self-Limited By Microvascular Clearance

Kha N. Le, PhD[1], **Chao-Wei Hwang, MD, PhD**[2], **A. Rami Tzafriri, PhD**[1], **Mark A. Lovich, MD, PhD**[3], **Alison Hayward, DVM**[4], and **Elazer R. Edelman, MD, PhD**[1,5]

[1]Harvard-MIT Division of Health Sciences and Technology, Massachusetts Institute of Technology, Cambridge, Massachusetts 02139

[2]Division of Cardiology, Department of Medicine, Johns Hopkins Hospital, Johns Hopkins School of Medicine, Baltimore, Maryland 21287

[3]Department of Anesthesiology and Pain Medicine, Caritas St. Elizabeth's Medical Center, Boston MA 02135

[4]Division of Comparative Medicine, Massachusetts Institute of Technology, Cambridge MA 02139

[5]Cardiovascular Division, Department of Medicine, Brigham and Women's Hospital, Harvard Medical School, Boston, Massachusetts 02115

Abstract

Background—The challenge of angiogenesis science is that stable sustained vascular regeneration in humans has not been realized despite promising preclinical findings. We hypothesized that angiogenic therapies powerfully self-regulate by dynamically altering tissue characteristics. Induced neocapillaries increase drug clearance and limit tissue retention and subsequent angiogenesis even in the face of sustained delivery.

Methods and Results—We quantified how capillary flow clears Fibroblast Growth Factor (FGF) following local epicardial delivery. FGF spatial loading was significantly reduced with intact coronary perfusion. Penetration and retention decreased with trans-endothelial permeability, a trend diametrically opposite to intravascular delivery, where factor delivery depends on vascular leak, but consistent with a continuum model of drug transport in perfused tissues. Model predictions of FGF sensitivity to manipulations of its diffusivity and trans-endothelial permeability were validated by conjugation to sucrose octasulfate (SOS). Induction of neocapillaries adds pharmacokinetic complexity. Sustained local FGF delivery *in vivo* produced a burst of neovascularization in ischemic myocardium but was followed by drug washout and a five-fold decrease in FGF penetration depth

Conclusions—The very efficacy of pro-angiogenic compounds enhances their clearance and abrogates their pharmacologic benefit. This self-limiting property of angiogenesis may explain the failures of promising pro-angiogenic therapies.

Keywords

angiogenesis; capillaries; growth substances; ischemia; pharmacokinetics

Correspondence should be addressed to: Kha N. Le Division of Health Sciences and Technology Massachusetts Institute of Technology Room E25-442 77 Massachusetts Avenue Cambridge, Massachusetts 02139 Phone: (617) 258-8901 Fax: (617) 253-2514 knle@mit.edu.

Disclosures None.

Introduction

Stimulation of neovascularization using angiogenic growth factors might reduce myocardial infarct size and improve cardiac function[1], and peripheral tissue[2] perfusion. Yet, impressive results in tissue culture and animal studies[3–7] have not been sustained in clinical trials[8–11]. Intravascular delivery of angiogenic factors is convenient but challenged by the requirements for high doses and long residence times[8, 10]. Cell and gene injections might provide a continuous source of growth factor, and intramyocardial or pericardial delivery have elevated local tissue drug concentrations with lower systemic exposure in animal models[12]. However, the promise of symptomatic improvement and increased capillary density seen in early clinical trials with intramyocardial injections of FGF after coronary artery bypass grafting[13] has not endured in larger clinical trials, and clinical outcomes in general with local growth factor delivery have been mixed[9, 14–18].

Some have postulated that myocardial growth factor concentrations and/or drug residence time were inadequate for sustained angiogenesis despite controlled release delivery[19]. However, the local pharmacokinetic processes governing uptake and distribution of growth factors in highly vascularized tissues such as myocardium remain ill-defined. It is therefore possible that the reverse is true and that growth factor concentrations were actually more than sufficient initially. We hypothesized that local delivery can induce neocapillary growth but in doing so changes the balance between drug delivery and microvascular drug clearance to favor the latter, such that the very pharmacologic efficacy of these compounds limits their biological effect.

We used a series of *ex vivo*, analytical and *in vivo* experimental animal models to quantify how growth factors distribute within vascularized tissue, and how neovascularization following delivery of angiogenic growth factors affects their pharmacokinetics and efficacy. These studies strongly suggest that angiogenesis is powerfully self-regulating as the capillaries induced by angiogenic drug therapy may increase clearance rates limiting tissue levels of growth factor and subsequent angiogenesis even with sustained delivery.

Methods

Ex-vivo Myocardial Drug Delivery with and without Perfusion

Sprague Dawley rats (0.5–0.6 kg) were anesthetized with 35 mg/kg ketamine and 5 mg/kg xylazine, and anticoagulated with 1000 U subcutaneous heparin prior to CO_2 euthanasia . The aorta was cannulated and heart retrograde perfused with cardioplegia (Osmolality $= 289$ mOsm/ $kgH_2O \pm 5\%$) composed of Krebs-Henseleit buffer (Sigma-Aldrich) with high potassium (30 mmol/L KCl) and 4 % BSA (Sigma-Aldrich) to establish diastolic arrest. The heart was excised and perfused at 95 mmHg. Coronary flow was monitored periodically and ranged 8–10 ml/ minutes throughout experiment. The perfusate was oxygenated by a foam bubble oxygenator with 95 % O_2 / 5 % CO_2 at 37°C. Samples were also examined in the absence of coronary perfusion to eliminate other effects. Here the aorta was cannulated and flushed with perfusate. As blood cleared from the circulation, coronary outflow from coronary sinus was stopped by clamping the right atrium and pulmonary artery ensuring myocardial capillaries patency and that the only difference between the control and perfused cases was coronary perfusion. The entire configuration resided within an enclosed box with 100 % humidity. We ascertained myocardial viability at 6 h by quantitatively documenting no additional tissue edema on H&E stained sections. Experimental protocols were in accordance with NIH guidelines for the humane care and use of laboratory animals and MIT committee on animal care.

Texas Red-FGF2 (TR-FGF2, 17 kDa, 5.88×10^{-2} μmol/L) or Texas Red labeled FGF2 conjugated to SOS complex (TR-(FGF2)$_2$-SOS complex, ~35 kDa, 2.86×10^{-2} μmol/L) were delivered to the rat myocardium from a drug-releasing chamber affixed to the anterior

epicardial surface by a cyanoacrylate based surgical adhesive (Glustitch). Heart were placed on a shaker at 100 RPM to ensure a well mixed epicardial drug source. A core of myocardial tissue in contact with and immediately adjacent to the drug source was harvested 6 h later using an 8 mm-diameter biopsy punch (Miltex). Tissue cores were cryo-sectioned (Leica CM1850) perpendicular to the epicardium for quantitative epifluorescence imaging (Leica DMRA2 microscope, Hamamatsu C4742-95 camera, MetaMorph software, Texas Red filter set). Since the fluorescent intensity of TR-FGF2 is linearly proportional to fluorophore[20], total drug deposition in the absence (M_{diff}) or the presence ($M_{diff\text{-}clear}$) of coronary perfusion were calculated by summing fluorescence intensities in the spatial distributions. Percent clearance of drug from coronary perfusion is

$$\%\text{clearance}=100 \times \left(1 - M_{diff-clear}/M_{diff}\right).$$

(Eq. M1)

In-vivo Myocardial Drug Delivery

Rabbits (New Zealand White, 3–3.5 kg) received an intramuscular injection of 35 mg kg^{-1} ketamine and 5 mg kg^{-1} of xylazine, and inhaled isoflurane anesthesia (1–3%) and positive pressure ventilation via a 3.0 mm endotracheal tube. The chest was shaved and sterilely prepared with Betadine and alcohol. A left thoracotomy was performed after local lidocaine injection. A clamp kept the chest open and a small opening in the pericardium was created with care to minimize pericardial damage. The left anterior descending coronary artery was ligated. Ischemia was confirmed by ST segment elevation on simultaneous continuous electrocardiography. Sodium alginate polymeric devices sustain-releasing ^{35}S-FGF1 from encapsulated heparin Sepharose beads (Supplemental Materials) were placed in the pericardial space and the percardiotomy suture repaired to prevent leakage. The thoracotomy and skin incision were closed. Positive end-expiratory pressure ventilation and a negative pressure chest tube prevented pneumothorax. Analgesia was with 0.03 mg kg^{-1} buprenorphine subcutaneous injections every 8 h for the first 72 h. Control animals received alginate encapsulated heparin Sepharose beads without FGF. Hearts were harvested 2, 8, 16 and 31 days after surgery, the aorta cannulated, flushed retrogradely with PBS, and snap-frozen in liquid nitrogen.

Quantification of in-vivo FGF1 and Blood Vessels Distribution

Two frozen myocardial cores were excised adjacent to the polymeric devices using an 8 mm diameter biopsy punch (Miltex). One core was mounted and cryosectioned (Leica CM1850) into 100 μm sections parallel to the epicardium. Sections were digested in 1 ml of Solvable tissue solubilizer (PerkinElmer) at 60°C overnight prior to radioactivity quantification (2500TR Liquid Scintillation Analyzer, Packard). The discrete spatial FGF1 concentration data were fit to the exponential profile implied by Eq. 4 (Table 1) using GraphPad software (Prism 5). The fit was used to estimate the penetration depth x_{90}, defined as distance from source to 90 % drop-off threshold, as $x_{90} = \ell \times ln(10)$. The other tissue core was cryo-sectioned into 10 μm thick sections in transmural direction. Sections were fixed for 5 m with 4 % paraformaldehyde (Electron Microscopy Sciences), washed for 30 s with cold acetone (Sigma-Aldrich), incubated in blocking serum (200 μl 1 % chicken serum, 1 h, 37°C), then in goat anti-PECAM-1 IgG (Santa Cruz Biotechnology, 200 μl of 1:50 dilution, 2 h, 37°C), washed three times in 0.1 % Tween 20 in PBS, incubated further with Alexa Fluor 488 chicken anti-goat IgG (Invitrogen, 200 μl 1:200 dilution, 2 h, 37°C), washed three times in Tween 20/PBS, cover-slip mounted, and imaged immediately with a fluorescence microscope (Leica DMRA2, FITC filter set). The images were thresholded to maximize the signal to noise ratio with Matlab (Mathworks, MA), yielding binary images of vessel distribution. Neovascular formation of tissue regions within 500 μm from epicardial source was quantified by computing the tissue area fraction stained by PECAM-1 (total number of pixels with PECAM-1 stain / total number of pixels of tissue area).

Statistical analysis

All data were presented as means ± s.e.m., except values for the clearance rate constants k which were reported as means ± propagated standard errors. Propagated errors s_k were calculated using the formula $\left(\dfrac{s_k}{k}\right)^2 = \left(\dfrac{s_D}{D}\right)^2 + 2\left(\dfrac{s_{x90}}{x_{90}}\right)^2$, where s_D and $S_{x_{90}}$ are standard errors for effective diffusivity D and penetration depth x_{90}, respectively. Statistical analyses were performed with the Student's t test where appropriate. P<0.05 (two-tailed) was considered statistically significant. Non-linear regression was performed using GraphPad software (Prism 5) to fit steady state spatial drug distributions to Eqs. S6 and S11 in obtaining values for clearance rate constant k and effective diffusivity D, respectively.

Results

FGF Distribution is Limited by Myocardial Perfusion

Drug transport through and deposition within tissues are governed by molecular weight-dependent processes such as diffusion and convection, and physicochemical attributes such as binding, partitioning, and metabolism[21–23]. We examined the effects of capillary perfusion on myocardial growth factor transport in rat hearts incubated at constant epicardial source concentrations (Fig. S1) with and without controlled coronary flow. When delivered to the *ex-vivo* myocardium in the absence of flow, TR-FGF2 distributed via diffusion to a penetration depth of 66 μm in 6 h (Fig 1). Restoration of coronary perfusion reduced TR-FGF2 penetration depth more than 2-fold to 28 μm, localizing growth factor closer to the epicardial drug source (Fig. 2).

Drug Diffusivity, Trans-endothelial Permeability and Vessel Density Influence Local Drug Distribution and Deposition

We examined the impact of coronary flow on drug penetration within the context of a continuum pharmacokinetics model of drug diffusion in the face of microvascular clearance (Eq. 1, Table 1). In the absence of perfusion the growth factor distribution curve mimics the analytical solution of the diffusion equation (Eq. 3, Table 1) with an apparent diffusivity of 0.021 ± 0.001 $\mu m^2 s^{-1}$ for TR-FGF2. This value is four orders of magnitude smaller than the reported diffusivity of FGF in free aqueous solution[24], reflecting the impact of steric hindrance and binding within tissues. TR is small (600 Da) and hydrophilic. Its diffusion is significantly higher than FGF in HSPG-rich myocardium and detected fluorescence is likely specific for TR-FGF-2. In the presence of coronary perfusion, the capacity of capillaries to clear drugs is restored and the distribution of TR-FGF2 at 6 h approaches an exponential steady state profile consistent with an apparent clearance rate constant $k = 1.15 \pm 0.06 \times 10^{-4}$ s^{-1} (Eq. 4, Table 1). Given a normal myocardial capillary density of ~ 12.9 %[25] and FGF2 aqueous diffusivity of 2.2×10^2 $\mu m^2 s^{-1}$ [24], our estimate of the clearance rate constant of FGF2 implies that trans-endothelial permeability and the permeability-to-diffusivity ratio are approximately 1.9×10^{-3} $\mu m s^{-1}$, and 8.8×10^{-6} μm^{-1}. This estimate is in line with the trans-endothelial permeability of a molecule with a molecular size of FGF2[26].

Analytic models of drug transport and loss to capillary flow were evaluated across a range of diffusivities, trans-endothelial permeabilities, and microvascular volume fractions. Steady state results (Eqs. S7 and S9, Supplemental Methods) were used as equilibrium is rapidly achieved. Penetration depth at steady state increases as the square root of the diffusion coefficient (Fig. 2a), and decreases as the square root of the trans-endothelial permeability constant (Fig. 2b). It is worth contrasting our results with those from *systemic* drug delivery through an intravascular route, where tissue absorption is proportional to trans-endothelial permeability. Increasing transvascular penetration in systemic delivery requires drugs that

permeate across the endothelium and interventions that increase, rather than decrease, vascular permeability[27–29]. Tissues with higher degrees of vascularization, as embodied by the vascular volume fraction, clear drugs faster and have lower steady state drug penetration (Fig. 2c). Thus, steady state drug penetration and distribution are highly dependent on drug diffusivity through tissue and net microvascular clearance, the compounded effect of trans-endothelial permeability and microvascular volume fraction (Eq. 2, Table 1).

The theoretical reduction in total deposition due to capillary clearance was calculated (Eq. 5, Table 1) and expressed as a function of the clearance rate constant k (Eqs. S8 and S12, Supplemental Methods). Percent clearance of drug with coronary perfusion is most sensitive for clearance rate constants ranging between 1×10^{-5} and 1×10^{-2} s^{-1} (Fig. 3a). Notably, our measurement of the clearance rate constant of TR-FGF2 falls within this range, suggesting that FGF clearance is highly sensitive to trans-endothelial permeability and microvascular volume fraction.

To examine whether the clearance rate constant of FGF might be modulated by altering its physicochemical properties, we used quantitative fluorescence imaging to contrast the distribution of TR-FGF2 alone or in association with SOS. SOS induces FGF dimerization and increases the effective molecular weight of TR-FGF2[30]. The increase in size was confirmed by size-exclusion chromatography, and should reduce trans-endothelial permeability, capillary washout, and effective diffusivity. Indeed, in the absence of coronary perfusion, TR-$(FGF2)_2$-SOS penetrated 40 % less than TR-FGF2 into the myocardium (40 μm, with an effective diffusivity of 0.013 ± 0.001 $μm^2s^{-1}$) reflecting its increased size ($D_{eff\ TR-FGF} = 0.021 \pm 0.001$ $μm^2s^{-1}$, Fig. 1 vs. Fig. 3b). But the larger compound was also less affected by coronary perfusion, with penetration depth falling only 26 % to 30 μm and total deposition falling by only 12 % (Fig. 3b). The muted sensitivity of TR-$(FGF2)_2$-SOS to flow is consistent with the estimated clearance rate constant ($k=4.37 \pm 0.33 \times 10^{-5}$ s^{-1}), model predictions (Fig 3a), and our hypothesis that larger molecules enter capillaries less readily.

In-vivo Angiogenic Response Limits Drug Distribution

Conventional pharmacokinetic models for drug distribution do not take into account the potential that drugs can alter capillary density, trans-endothelial permeability or drug clearance. Yet, angiogenic growth factors such as FGF1 and FGF2 are specifically administered to induce capillary growth, and it would be unreasonable to assume that trans-endothelial permeability and drug clearance are not similarly modified. Induced neovascularization implies an increase in the density of blood capillaries that could provide negative feedback limiting growth factor tissue penetration (Fig 2c). Our analysis of myocardial drug transport suggests that FGF would be particularly sensitive to induced capillary washout (Figs. 1 and 3a). We tested this hypothesis *in vivo* using radiolabeled FGF1 (^{35}S-FGF1). TR-FGF2 could not be used *in vivo* as its labeling intensity is much lower than that of ^{35}S-FGF1, rendering it virtually transparent at the doses delivered. Notably, ex-vivo experiments with ^{35}S-FGF1 were well explained by the diffusion-clearance model, and suggest that the transport parameters estimated for TR-FGF2 is similar to those of ^{35}S-FGF1 (Supplement).

Heparin-bound biologically active ^{35}S-FGF1 fractions were isolated, incorporated into heparin Sepharose-alginate wafers which sustain-release FGF1 for over 30 days *in vitro* and *in vivo* (Fig. 4b), and implanted in the pericardial space of ischemic rabbit hearts (Fig. 4a). FGF1 successfully penetrated 442 ± 91 μm into the myocardium over the first two days after release initiation. Yet, despite sustained delivery, penetration regressed over time falling 5-fold by day 8 (81 ± 30 μm), and remained low through day 31 (Fig. 5a). Enhanced growth factor clearance was associated with the induction of neovasculature. Two days after device implantation the fraction of PECAM-1 stained tissue was 56 % greater in animals receiving FGF1 (4.4 %) compared to baseline density (2.8 %) in control animals with identical devices devoid of growth

factor (P < 0.05, Fig. 5c). Neovascularization peaked at day 8 (8.7 %) doubled that from day 2 (P < 0.01, Fig. 5c), coinciding with the drop in drug distribution. Similarly, the fraction of PECAM-1 stained tissue decreased significantly from day 8 to day 31 (−62 % P < 0.01, Fig. 5c), most likely from regression of neocapillaries as the concentration of FGF1 becomes sub-therapeutic. Examination of drug delivery devices for remaining drug content confirmed that the decreasing myocardial concentrations arose from increasing capillary clearance rather than decreasing drug delivery. None of the delivery devices were depleted of drug, and all continued to release drug with constant flux (Fig. 4b) following the expected burst release of ~37.5 % during the first 6 h.

Discussion

The potential of angiogenic promoters of endothelial cell growth and neovascularization is well established in cell and tissue culture [31, 32]. Yet, angiogenic growth factors have yet to produce stable sustained angiogenesis in clinical trials[8, 10]. While there are undoubtedly biological factors involved[33], our study suggests that fundamental transport barriers and particularly the self-limiting pharmacokinetics of angiogenic therapy also may impair the realization of sustained neovascularization.

Our results reveal that drug trans-endothelial permeability plays a vital role in governing drug distribution. Lower trans-endothelial permeability ensures greater myocardial drug penetration following local application (Fig. 2b). FGF is an arterial vasodilator but this cannot explain our results as expected changes in arteriolar volume[34] could not reach the scale of our results or explain the difference in growth factor distribution between perfused and static flow conditions which both saw growth factor. The dependence of drug distribution on trans-endothelial permeability and capillary density takes on further complexity for angiogenic compounds that can remodel their tissue environment. Over the course of treatment, vessel density in ischemic tissues increases in FGF1-laden tissue regions (within 500–600 μm depth from epicardium, Fig 5b). Indeed, abundant neovascularization occurs from day 2 to 8, but drug washout rises as well precipitously dropping the local tissue concentration of FGF1 (Fig 5a) and penetration depth of FGF1, despite no quantifiable change in growth factor delivery. FGF1's instability in the absence of heparin[35] cannot account for the observed effects, as the factor was released directly from the heparin Sepharose devices to the epicardial tissue. Released FGF1 likely binds reversibly to myocardial HSPGs prolonging its tissue half-life. Indeed, angiogenic activity was observed 8 days after delivery (Fig 5). Moreover, changes in angiogenic action correlated with regression of FGF1 distribution, not a decrease in activity or stability. Continuum pharmacokinetics (Eq. S15, Supplemental Methods) suggest a 5-fold increase in capillary washout between days 2–8. Such an increase in the FGF1 clearance could arise from an increase in microvascular density and/or trans-endothelial permeability (Eq. 2, Table 1). The observed 65 % rise in capillary density between days 2 and 8 indicates that the latter plays a dominant role and suggests that the induced vasculature is immature and highly permeable to FGF1.

Our findings, therefore, offer possibilities for engineering drugs to penetrate tissue better by reducing their trans-endothelial permeability. FGF2 lies within the region where drug penetration depth is highly sensitive to the clearance rate constant k (Fig. 4a) which is directly proportional to trans-endothelial permeability (Eq. 2, Table 1), whereas $(FGF2)_2$-SOS with its 2.6 times lower clearance is less affected by flow. More than 50 % of FGF2 is cleared by coronary perfusion, but only 12 % for $(FGF2)_2$-SOS (Fig. 1 vs. Fig. 3b). Therefore, one way to decrease permeability is to consider drugs of higher molecular weight. While higher molecular weight implies lower myocardial drug diffusivity, the ratio of permeability to diffusivity can drop two orders of magnitude as molecular radius increases from 2.4 to 36 Å [26]. A different method for modulating trans-endothelial permeability is by modification of drug

charge. Indeed, it has been shown that negatively charged dextrans exhibit 10 times lower trans-endothelial permeability than neutral analogs[36]. This approach may present a method for lowering trans-endothelial permeability of a drug to increase penetration depth and deposition.

Our study also highlights the impact of capillary clearance on myocardial drug distribution and elimination, and sets a ceiling for the depth of drug penetration at steady state. Such clearance is dependent on the trans-endothelial permeability of the delivered drug, and tissue vascularity. At normal arterial pO_2, a significant portion of capillaries is relatively constricted. Normal myocardium can respond swiftly to arterial hypoxia through active hyperemia by dilating capillaries and effectively decreasing intercapillary distance and thus oxygen diffusion barrier[37]. Through reactive hyperemia the glycocalyx lining of endothelial cells can be modified by reactive oxygen species to increase transendothelial permeability, and capillary and postcapillary venule diameter[38]. However, myocardial capillary density declines markedly with ischemia and infarction, limiting capillary reserve[39–41]. Because capillaries act as spatially distributed sinks to drug, myocardium with denser functional vasculature will clear drug more efficiently and rapidly, creating zones of low drug concentration. Gradation in vascularity in diseased tissue thus has important consequences for local drug delivery. Since capillary flow in ischemic and infarcted regions is substantially lower than in normal tissue, our data predict that drug penetration would be greater. Placing delivery devices directly in the ischemic region should confer the pharmacokinetic advantages of decreased capillary washout; in well-perfused regions, drug molecules may never reach ischemic areas at sufficient levels. Pericardial delivery of growth factors to target endocardial ischemic regions may thus prove futile since drugs will not easily cross well-perfused epicardial regions. Indeed, drug penetration in the presence of capillary perfusion was limited *ex vivo* (Fig. 1) and *in vivo* (Fig. 5) despite ample time for distant diffusion.

The integrated studies presented suggest that angiogenesis is powerfully self-regulating as the very capillaries induced by angiogenic drug therapy may increase clearance as well. The pharmacodynamic changes during the early angiogenic therapy can tip the pharmacokinetics to conditions that are unfavorable for growth factor penetration, which in turn affects long term therapeutic goals. This mechanism implies a natural upper limit effect for pharmacologic revascularization which restricts angiogenic drug penetration and spatially confines the sprouting of new vessels near the drug source. At day 31, the FGF1 level in the 100–500 μm tissue region falls to undetectable levels, and significant regression of neovascularization consequently occurs in the absence of local growth factor (Fig 5c). One might well imagine that such forces are essential to endogenous regulation of tissue morphogenesis and repair, and that loss of such regulation may help explain the growth of vascular tumors, and other arterial-venous malformations and anomalies.

The interdependence of the pharmacokinetics and pharmacodynamics elucidated in this study may explain the difficulty of realizing the clinical potential of angiogenic compounds and suggests that efficacy becomes critically dependent on device placement and drug's trans-endothelial permeability. The quantitative framework presented here may help guide rational selection of angiogenic compounds based on a favorable physicochemical profile, and drug delivery strategies that take advantage of the regulation between growth factor pharmacokinetics and angiogenic pharmacodynamics.

Clinical summary

Pro-angiogenic growth factors have long been considered for regenerating ischemic tissues. Yet, sustained clinical benefit has not followed promising preclinical findings even with advances in local delivery technology. Quantitative and animal models suggest that the limited late efficacy of local delivery of angiogenic factors stems partly from the very early

success at inducing vessel growth. Fibroblast Growth Factor (FGF) released from a polymeric implant penetrates ischemic rabbit myocardium in vivo for the first two days of local delivery and indeed induces neovascularization. But as new vessels are formed drug is cleared rapidly, and the induced vessel mass regresses. As each wave of new vessels appears in response to the angiogenic factor pools, the factors are cleared and the angiogenic signal abates as a receding wave that implodes back towards the growth factor source. Despite a constantly eluting source of FGF, the front of new vessels continues to fall back. Eight days after release initiation neovascularization remains but only as a regressed zone immediately around the delivery device. By day 30 there is only a superficial layer of vessels around the release device.

This interdependence of pharmacokinetics and pharmacodynamics may explain the difficulty of realizing sustained clinical angiogenesis with local release and suggests that efficacy depends on device placement and drug trans-endothelial permeability. The quantitative framework presented here may help guide rational selection of specific angiogenic compounds based on a favorable physicochemical profile, and drug delivery strategies that take advantage of the tight regulation between growth factor pharmacokinetics and angiogenic pharmacodynamics.

Supplementary Material

Refer to Web version on PubMed Central for supplementary material.

Acknowledgments

References

1. Yanagisawa-Miwa A, Uchida Y, Nakamura F, Tomaru T, Kido H, Kamijo T, Sugimoto T, Kaji K, Utsuyama M, Kurashima C. Salvage of infarcted myocardium by angiogenic action of basic fibroblast growth factor. Science 1992;257:1401–1403. [PubMed: 1382313]

2. Takeshita S, Pu LQ, Stein LA, Sniderman AD, Bunting S, Ferrara N, Isner JM, Symes JF. Intramuscular administration of vascular endothelial growth factor induces dose-dependent collateral artery augmentation in a rabbit model of chronic limb ischemia. Circulation 1994;90:II228–234. [PubMed: 7525111]

3. Harada K, Friedman M, Lopez JJ, Wang SY, Li J, Prasad PV, Pearlman JD, Edelman ER, Sellke FW, Simons M. Vascular endothelial growth factor administration in chronic myocardial ischemia. Am J Physiol 1996;270:H1791–1802. [PubMed: 8928888]

4. Lopez JJ, Edelman ER, Stamler A, Hibberd MG, Prasad P, Thomas KA, DiSalvo J, Caputo RP, Carrozza JP, Douglas PS, Sellke FW, Simons M. Angiogenic potential of perivascularly delivered aFGF in a porcine model of chronic myocardial ischemia. Am J Physiol 1998;274:H930–936. [PubMed: 9530206]

5. Montesano R, Vassalli JD, Baird A, Guillemin R, Orci L. Basic fibroblast growth factor induces angiogenesis in vitro. Proc Natl Acad Sci U S A 1986;83:7297–7301. [PubMed: 2429303]

6. Unger EF, Banai S, Shou M, Lazarous DF, Jaklitsch MT, Scheinowitz M, Correa R, Klingbeil C, Epstein SE. Basic fibroblast growth factor enhances myocardial collateral flow in a canine model. Am J Physiol 1994;266:H1588–1595. [PubMed: 8184938]

7. Watanabe E, Smith DM, Sun J, Smart FW, Delcarpio JB, Roberts TB, Van Meter CH Jr. Claycomb WC. Effect of basic fibroblast growth factor on angiogenesis in the infarcted porcine heart. Basic Res Cardiol 1998;93:30–37. [PubMed: 9538935]

8. Simons M, Annex BH, Laham RJ, Kleiman N, Henry T, Dauerman H, Udelson JE, Gervino EV, Pike M, Whitehouse MJ, Moon T, Chronos NA. Pharmacological treatment of coronary artery disease with recombinant fibroblast growth factor-2: double-blind, randomized, controlled clinical trial. Circulation 2002;105:788–793. [PubMed: 11854116]

9. Rajagopalan S, Mohler ER 3rd, Lederman RJ, Mendelsohn FO, Saucedo JF, Goldman CK, Blebea J, Macko J, Kessler PD, Rasmussen HS, Annex BH. Regional angiogenesis with vascular endothelial growth factor in peripheral arterial disease: a phase II randomized, double-blind, controlled study of adenoviral delivery of vascular endothelial growth factor 121 in patients with disabling intermittent claudication. Circulation 2003;108:1933–1938. [PubMed: 14504183]

10. Henry TD, Annex BH, McKendall GR, Azrin MA, Lopez JJ, Giordano FJ, Shah PK, Willerson JT, Benza RL, Berman DS, Gibson CM, Bajamonde A, Rundle AC, Fine J, McCluskey ER. The VIVA trial: Vascular endothelial growth factor in Ischemia for Vascular Angiogenesis. Circulation 2003;107:1359–1365. [PubMed: 12642354]

11. Gyongyosi M, Khorsand A, Zamini S, Sperker W, Strehblow C, Kastrup J, Jorgensen E, Hesse B, Tagil K, Botker HE, Ruzyllo W, Teresinska A, Dudek D, Hubalewska A, Ruck A, Nielsen SS, Graf S, Mundigler G, Novak J, Sochor H, Maurer G, Glogar D, Sylven C. NOGA-guided analysis of regional myocardial perfusion abnormalities treated with intramyocardial injections of plasmid encoding vascular endothelial growth factor A-165 in patients with chronic myocardial ischemia: subanalysis of the EUROINJECT-ONE multicenter double-blind randomized study. Circulation 2005;112:I157–165. [PubMed: 16159809]

12. Lazarous DF, Shou M, Stiber JA, Dadhania DM, Thirumurti V, Hodge E, Unger EF. Pharmacodynamics of basic fibroblast growth factor: route of administration determines myocardial and systemic distribution. Cardiovasc Res 1997;36:78–85. [PubMed: 9415275]

13. Laham RJ, Chronos NA, Pike M, Leimbach ME, Udelson JE, Pearlman JD, Pettigrew RI, Whitehouse MJ, Yoshizawa C, Simons M. Intracoronary basic fibroblast growth factor (FGF-2) in patients with severe ischemic heart disease: results of a phase I open-label dose escalation study. J Am Coll Cardiol 2000;36:2132–2139. [PubMed: 11127452]

14. Hedman M, Hartikainen J, Syvanne M, Stjernvall J, Hedman A, Kivela A, Vanninen E, Mussalo H, Kauppila E, Simula S, Narvanen O, Rantala A, Peuhkurinen K, Nieminen MS, Laakso M, Yla-Herttuala S. Safety and feasibility of catheter-based local intracoronary vascular endothelial growth factor gene transfer in the prevention of postangioplasty and in-stent restenosis and in the treatment of chronic myocardial ischemia: phase II results of the Kuopio Angiogenesis Trial (KAT). Circulation 2003;107:2677–2683. [PubMed: 12742981]

15. Lederman RJ, Mendelsohn FO, Anderson RD, Saucedo JF, Tenaglia AN, Hermiller JB, Hillegass WB, Rocha-Singh K, Moon TE, Whitehouse MJ, Annex BH. Therapeutic angiogenesis with recombinant fibroblast growth factor-2 for intermittent claudication (the TRAFFIC study): a randomised trial. Lancet 2002;359:2053–2058. [PubMed: 12086757]

16. Makinen K, Manninen H, Hedman M, Matsi P, Mussalo H, Alhava E, Yla-Herttuala S. Increased vascularity detected by digital subtraction angiography after VEGF gene transfer to human lower limb artery: a randomized, placebo-controlled, double-blinded phase II study. Mol Ther 2002;6:127–133. [PubMed: 12095313]

17. Stewart DJ, Hilton JD, Arnold JM, Gregoire J, Rivard A, Archer SL, Charbonneau F, Cohen E, Curtis M, Buller CE, Mendelsohn FO, Dib N, Page P, Ducas J, Plante S, Sullivan J, Macko J, Rasmussen C, Kessler PD, Rasmussen HS. Angiogenic gene therapy in patients with nonrevascularizable ischemic heart disease: a phase 2 randomized, controlled trial of AdVEGF(121) (AdVEGF121) versus maximum medical treatment. Gene Ther 2006;13:1503–1511. [PubMed: 16791287]

18. van Royen N, Schirmer SH, Atasever B, Behrens CY, Ubbink D, Buschmann EE, Voskuil M, Bot P, Hoefer I, Schlingemann RO, Biemond BJ, Tijssen JG, Bode C, Schaper W, Oskam J, Legemate DA, Piek JJ, Buschmann I. START Trial: a pilot study on STimulation of ARTeriogenesis using subcutaneous application of granulocyte-macrophage colony-stimulating factor as a new treatment for peripheral vascular disease. Circulation 2005;112:1040–1046. [PubMed: 16087795]

19. Gounis MJ, Spiga MG, Graham RM, Wilson A, Haliko S, Lieber BB, Wakhloo AK, Webster KA. Angiogenesis is confined to the transient period of VEGF expression that follows adenoviral gene delivery to ischemic muscle. Gene Ther 2005;12:762–771. [PubMed: 15772688]

20. Lakowicz, JR. Principles of fluorescence spectroscopy. Vol. 3rd ed.. Springer; New York: 2006.

21. Edelman ER, Lovich M. Drug delivery models transported to a new level. Nat Biotechnol 1998;16:136–137. [PubMed: 9487512]

22. Hwang CW, Wu D, Edelman ER. Physiological transport forces govern drug distribution for stent-based delivery. Circulation 2001;104:600–605. [PubMed: 11479260]

23. Baxter LT, Jain RK. Transport of fluid and macromolecules in tumors. III. Role of binding and metabolism. Microvasc Res 1991;41:5–23. [PubMed: 2051954]

24. Filion RJ, Popel AS. A reaction-diffusion model of basic fibroblast growth factor interactions with cell surface receptors. Ann Biomed Eng 2004;32:645–663. [PubMed: 15171620]

25. Wacker CM, Bauer WR. Myocardial microcirculation in humans--new approaches using MRI. Herz 2003;28:74–81. [PubMed: 12669220]

26. Michel CC, Curry FE. Microvascular permeability. Physiol Rev 1999;79:703–761. [PubMed: 10390517]

27. Dreher MR, Liu W, Michelich CR, Dewhirst MW, Yuan F, Chilkoti A. Tumor vascular permeability, accumulation, and penetration of macromolecular drug carriers. J Natl Cancer Inst 2006;98:335–344. [PubMed: 16507830]

28. Lejeune FJ. Clinical use of TNF revisited: improving penetration of anti-cancer agents by increasing vascular permeability. J Clin Invest 2002;110:433–435. [PubMed: 12189235]

29. Siegal T, Zylber-Katz E. Strategies for increasing drug delivery to the brain: focus on brain lymphoma. Clin Pharmacokinet 2002;41:171–186. [PubMed: 11929318]

30. Herr AB, Ornitz DM, Sasisekharan R, Venkataraman G, Waksman G. Heparin-induced self-association of fibroblast growth factor-2. Evidence for two oligomerization processes. J Biol Chem 1997;272:16382–16389. [PubMed: 9195945]

31. Dinbergs ID, Brown L, Edelman ER. Cellular response to transforming growth factor-beta1 and basic fibroblast growth factor depends on release kinetics and extracellular matrix interactions. J Biol Chem 1996;271:29822–29829. [PubMed: 8939921]

32. Nabel EG, Yang ZY, Plautz G, Forough R, Zhan X, Haudenschild CC, Maciag T, Nabel GJ. Recombinant fibroblast growth factor-1 promotes intimal hyperplasia and angiogenesis in arteries in vivo. Nature 1993;362:844–846. [PubMed: 7683112]

33. Cao R, Brakenhielm E, Pawliuk R, Wariaro D, Post MJ, Wahlberg E, Leboulch P, Cao Y. Angiogenic synergism, vascular stability and improvement of hind-limb ischemia by a combination of PDGF-BB and FGF-2. Nat Med 2003;9:604–613. [PubMed: 12669032]

34. Wu HM, Yuan Y, McCarthy M, Granger HJ. Acidic and basic FGFs dilate arterioles of skeletal muscle through a NO-dependent mechanism. Am J Physiol 1996;271:H1087–1093. [PubMed: 8853345]

35. Rosengart TK, Kuperschmid JP, Maciag T, Clark RE. Pharmacokinetics and distribution of heparin-binding growth factor I (endothelial cell growth factor) in the rat. Circ Res 1989;64:227–234. [PubMed: 2463884]

36. Elmalak O, Lovich MA, Edelman E. Correlation of transarterial transport of various dextrans with their physicochemical properties. Biomaterials 2000;21:2263–2272. [PubMed: 11026632]

37. Martini J, Honig CR. Direct measurement of intercapillary distance in beating rat heart in situ under various conditions of O 2 supply. Microvasc Res 1969;1:244–256. [PubMed: 5406306]

38. Rubio-Gayosso I, Platts SH, Duling BR. Reactive oxygen species mediate modification of glycocalyx during ischemia-reperfusion injury. Am J Physiol Heart Circ Physiol 2006;290:H2247–2256. [PubMed: 16399871]

39. McDonagh PF, Cohen DM, Suaudeau J, Laks H. The effects of myocardial ischemia followed by reperfusion on perfused coronary capillarity. Microcirc Endothelium Lymphatics 1985;2:67–84. [PubMed: 3836337]

40. Van Kerckhoven R, van Veghel R, Saxena PR, Schoemaker RG. Pharmacological therapy can increase capillary density in post-infarction remodeled rat hearts. Cardiovasc Res 2004;61:620–629. [PubMed: 14962492]

41. Xie Z, Gao M, Batra S, Koyama T. The capillarity of left ventricular tissue of rats subjected to coronary artery occlusion. Cardiovasc Res 1997;33:671–676. [PubMed: 9093538]
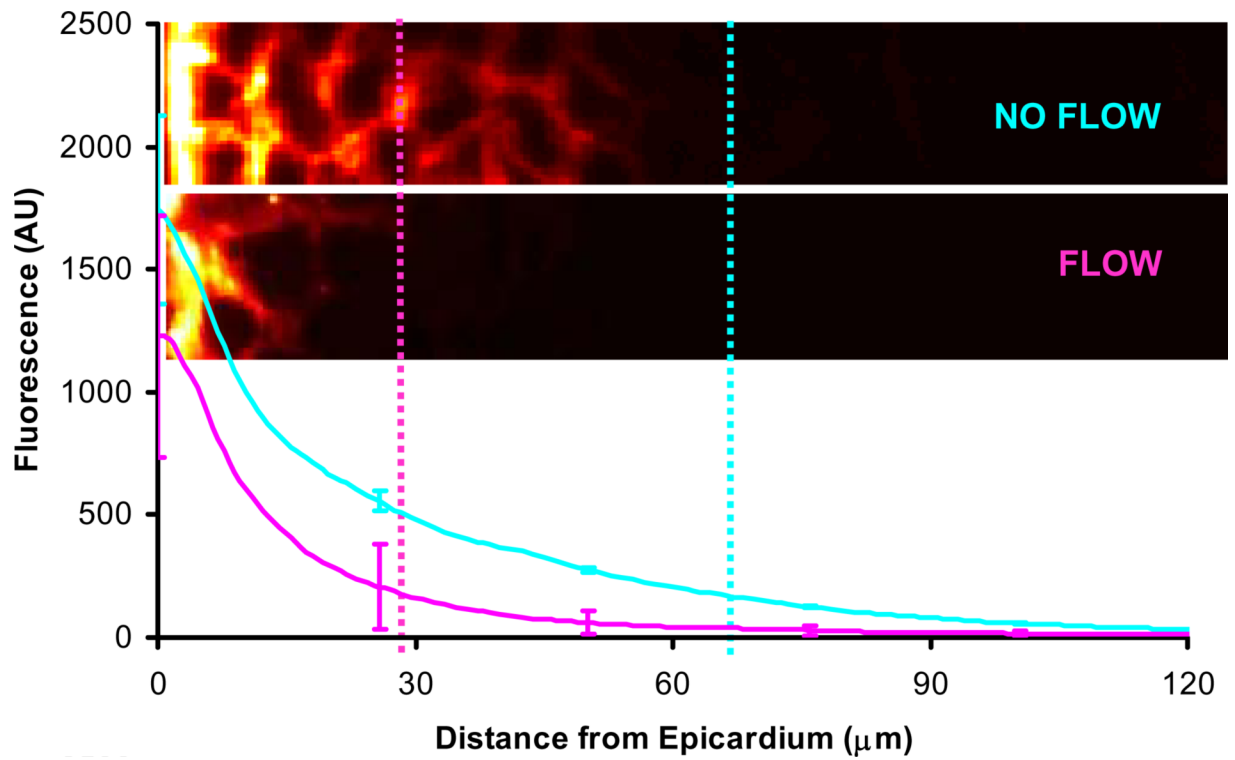
FIGURE 1. Myocardial Capillary perfusion Impedes Drug Penetration
Distribution and representative fluorescence microscopy images of TR-FGF2 in rat
myocardium with (magenta) and without coronary perfusion (blue). Data represent mean ±
s.e.m. (n=3). Penetration depth (x_{90}) is estimated as the location of the 90 % drop-off from the
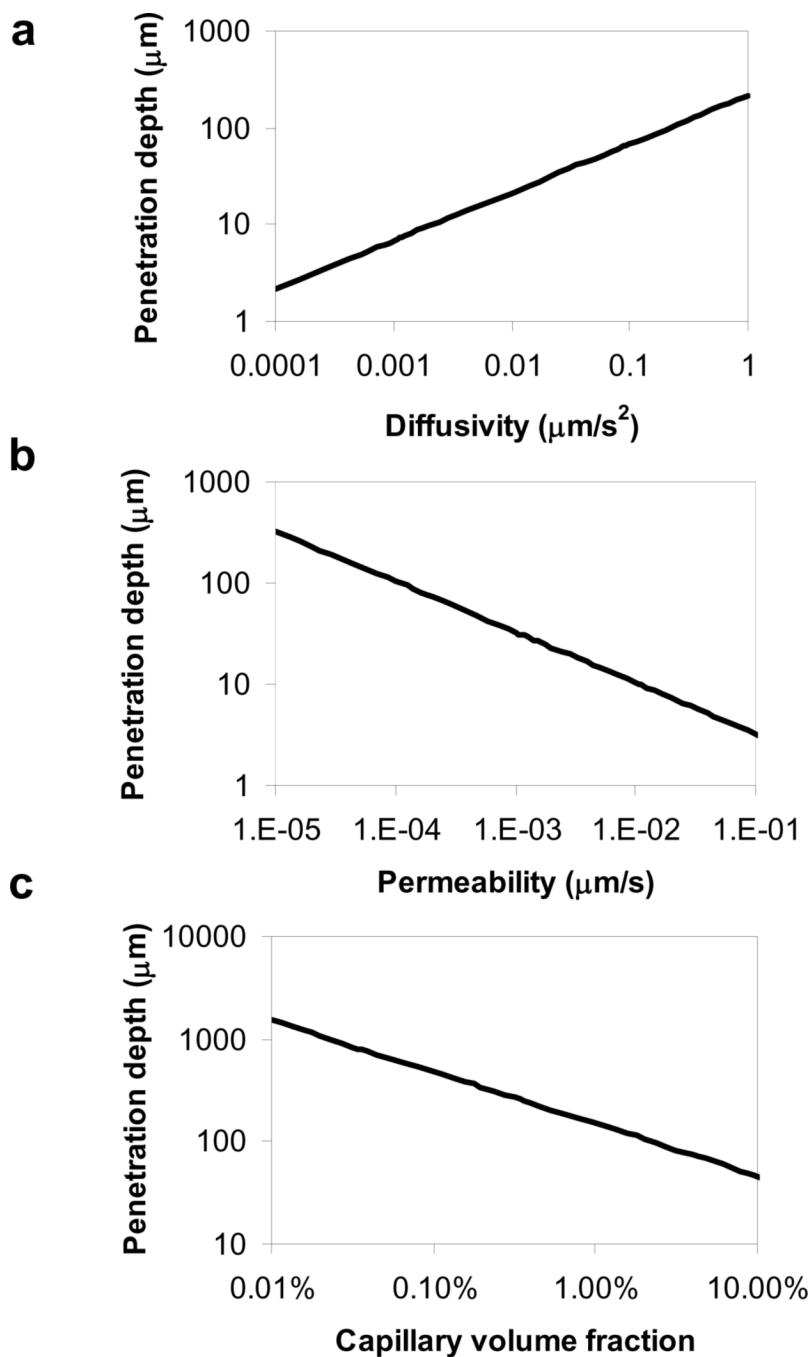threshold (vertical dashed lines).

FIGURE 2. Continuum Pharmacokinetic Model
Penetration depth x_{90}, defined as distance from source to 90 % drop-off threshold, $x_{90} = \ell \times ln$ *(10)*, where ℓ is calculated based on Eq. 4 (Table 1), is expressed as a function of drug diffusivity (a), trans-endothelial permeability (b), and capillary volume fraction (c). Parameter values cover a range of two orders of magnitude below to above those of FGF2 in the heart. FGF2 diffusivity = 0.02 $\mu m^2 s^{-1}$ and clearance constants k were empirically verified, and trans-endothelial permeability derived from Eq. 2 (Table 1). Capillary volume fraction (ϕ_{mv}) was varied over 3 log orders between the extremes of ischemic and normal tissue vascularity[25].

These relationships are linear in log-log scale axes, demonstrating adherence to power law functions.

a
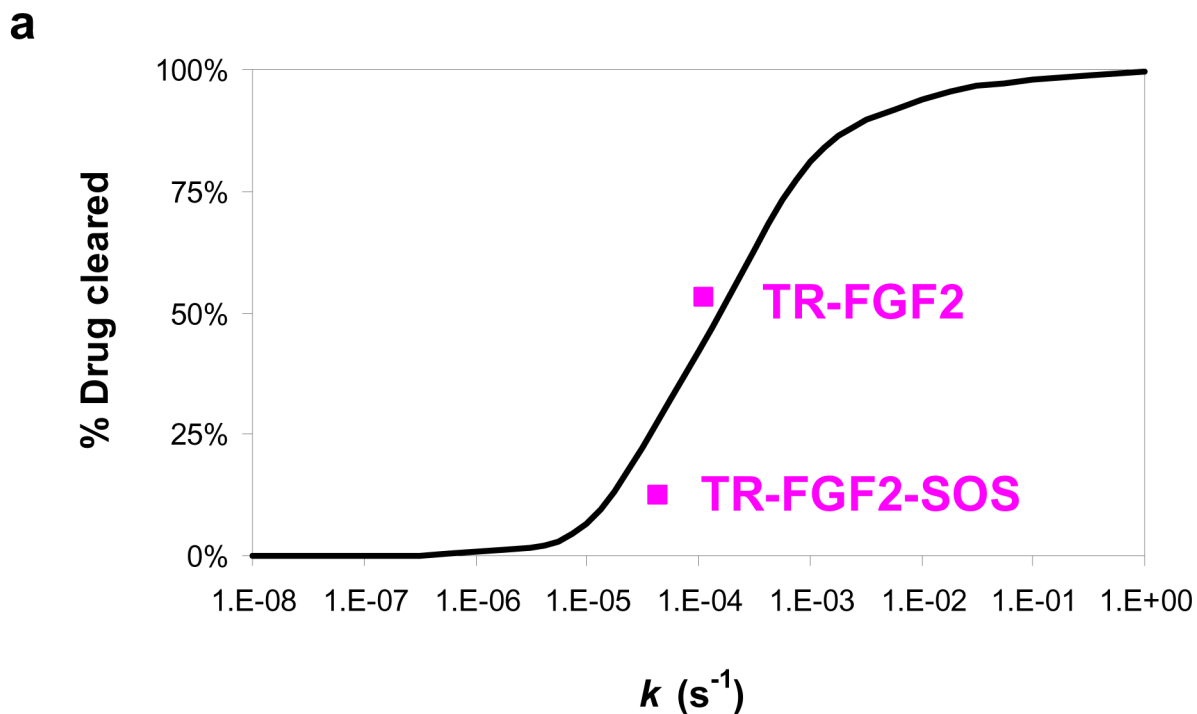
b
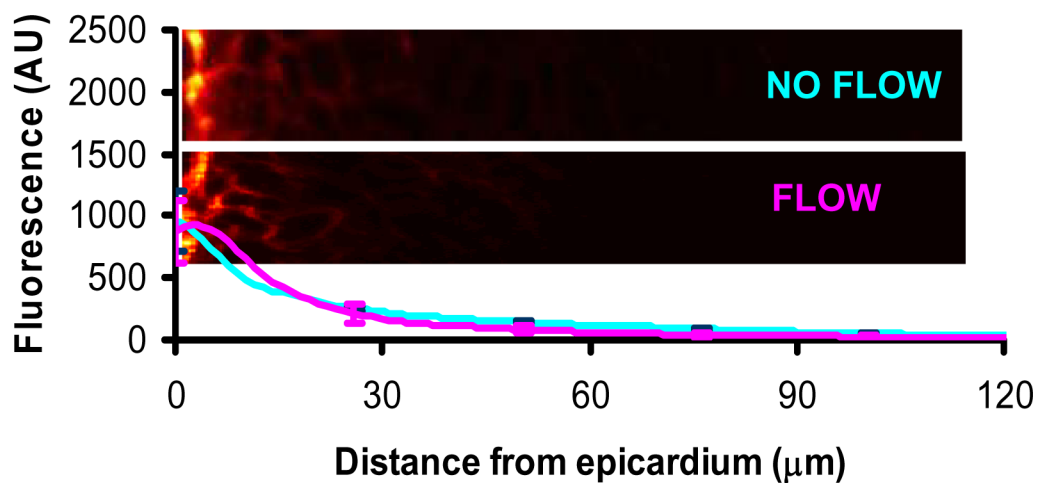
Texas red-FGF2-SOS dimer

FIGURE 3. FGF Distribution is Sensitive to Alteration in Drug Clearance
(a) Percent drug cleared by capillaries calculated using the analytical model (Eq. 5, Table 1) as a function of clearance rate constant k (black line). Experimental data points for TR-FGF2 and TR-(FGF2)$_2$-SOS analyzed by Eq. M1 (Methods) are superimposed (magenta squares) on model predictions providing perspective on the sensitivity of FGF2 to manipulation of its clearance constant. (b) Distribution and representative fluorescence microscopy images of TR-(FGF2)$_2$-SOS in rat myocardium with coronary perfusion (magenta) and without coronary perfusion (blue). Data represent mean ± s.e.m. (n=3).
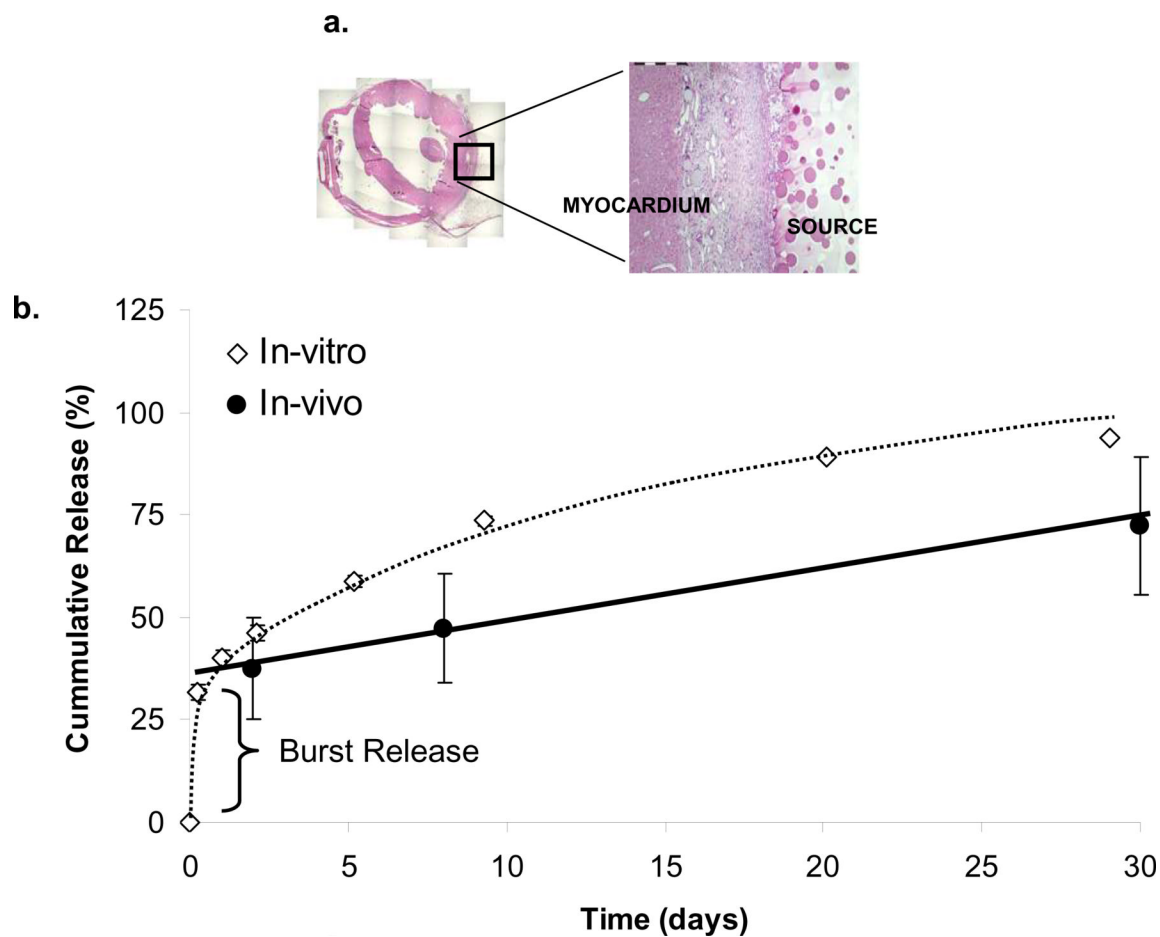
a.

b.

FIGURE 4. Polymeric Devices Sustain Release FGF1 over 30 days
(a) Cross sectional area of H&E stained rabbit myocardial tissue shows location of drug release source (adjacent to left ventricular free wall) and interface between drug source and myocardium. (b) Percentage of cumulative ^{35}S-FGF1 released into PBS buffer *in-vitro* (white diamonds, data represent mean ± s.e.m. (n=10), 100% corresponds to approximately 90μg ^{35}S-FGF1 per circular disk of 8mm diameter and 1mm thickness), and throughout *in-vivo* experiment (black circles, data represent mean ± s.e.m. (n=3), 100% corresponds to approximately 450 μg ^{35}S-FGF1 per device (20mm × 20mm × 1mm) for in-vivo experiments), calculated by % drug released = (total drug within source – total drug remaining)/ total drug within source × 100 %.
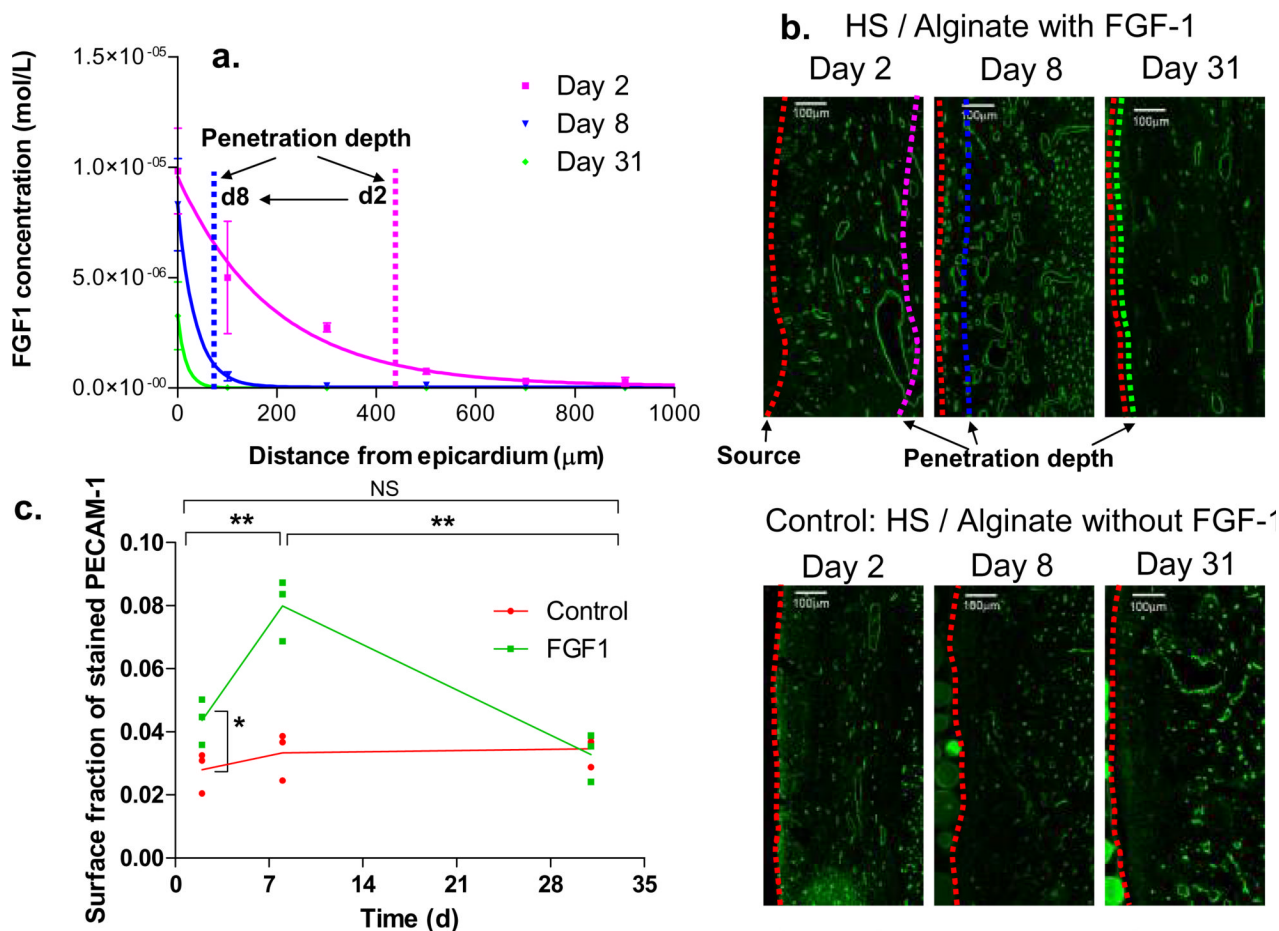
FIGURE 5. In-vivo Ischemic Heart Model
(a) Spatial distributions of tissue S^{35}-FGF1 concentration at days 2, 8, and 31 following coronary ligation and implantation of sustained release source. FGF1 was quantified using liquid scintillation counting following serial sectioning. Data represent mean ± s.e.m. (n=3) (b) Representative fluorescent images of PECAM-1 labeled blood vessels in tissue regions adjacent to drug source for experimental animals receiving heparin-Sepharose beads / alginate source with S^{35}-FGF1 and control animals receiving devices without FGF1. Dashed red line on the right edge denotes interface between source and epicardium. Magenta, blue and green dashed lines represent the penetration depth at 90 % drop-off threshold from tissue/source interface calculated from spatial S^{35}-FGF1 distributions. (c) Vascular to tissue surface fraction (calculated by normalizing total number of pixels stained by PECAM-1 to total tissue area within 500 μm depth from source) is expressed as a function of time. Scale bars represent 100 μm. Data points represent PECAM-1 stained surface fraction of individual hearts (n=3), and connecting lines denote trend of mean value. * denotes P < 0.05. ** denotes P < 0.01 (P = 0.007 between days 2 and 8, and P = 0.003 between days 8 and 31).

TABLE 1

Continuum Pharmacokinetic Model Equations for Epicardial Drug Delivery

Detailed derivations are included in Supplemental Methods. Eq. 1 describes the transport of drug in the presence of capillary clearance. C represents drug concentration in the tissue as a function of time t, distance from the epicardium x, diffusivity D and apparent clearance constant k. Eq. 2 relates the apparent clearance constant k to capillary permeability P_{mv}, capillary volume fraction ϕ_{mv} and capillary diameter R_{mv}. Eq. 3 describes steady state tissue concentration normalized to source concentration C_o in the absence of capillary perfusion. Eq. 4 shows the steady state tissue concentration in the presence of capillary perfusion, where ℓ is drug penetration depth. Eq. 5 shows the percent drug clearance by capillary perfusion as a function of k and D.

Eq. 1	$\dfrac{\partial C}{\partial t} - D\dfrac{\partial^2 C}{\partial x^2} = -kC$
Eq. 2	$k = \left(\dfrac{2}{R_{mv}}\right)\dfrac{P_{mv}\phi_{mv}}{1-\phi_{mv}}$
Eq. 3	$C / C_0 \approx \mathrm{erfc}\left(\dfrac{x}{2\sqrt{Dt}}\right)$
Eq. 4	$C = C_0 e^{-x/\ell},\ \ell = \sqrt{\dfrac{D}{k}}$
Eq. 5	$\%\ \mathrm{clearance} = 100 \times \left[1 - \dfrac{\ell\,\mathrm{erf}(\sqrt{kt})}{\sqrt{4Dt/\pi}}\right]$